Proceedings of the ASME Summer Heat Transfer Conference
HT2008
August 10-14, 2008, Jacksonville, Florida, USA

HT2008-56446

FORMULATION OF FILM THEORY EQUATIONS FOR MODELING OF CONDENSATION OF STEAM-AIR MIXTURES IN A SHELL AND TUBE CONDENSER

Yousef Haseli, Ibrahim Dincer, Greg F. Naterer

University of Ontario Institute of Technology, Faculty of Engineering and Applied Science
2000 Simcoe Street North, Oshawa, Ontario, Canada, L1H 7K4
E-mails: yousef.haseli@uoit.ca, ibrahim.dincer@uoit.ca, greg.naterer@uoit.ca

ABSTRACT

Through development of the fundamental equations of Film Theory, condensation of steam in the presence of air in a horizontal counter-current shell and one-path tube condenser is modeled. The interaction between heat and mass transfer and hydrodynamics in the shell-side is taken into consideration. A comparison between the predictions of the model and a set of experimental data available in the archival literature indicates excellent accuracy of the new formulation. The accuracy of the method is further validated by generating profiles of the temperature and pressure drops of the gas flow through the baffles, at various air leakages. Additionally, the effects of air leakage and upstream cooling water temperature are investigated to determine how they influence the total condensation rate, shell-side gas temperature and pressure drops. The results show that the total condensation rate decreases 5% and 20.5% for an air leakage of 1% and 5%, respectively, compared to the situation of pure vapor. Also, increasing the inlet cooling water temperature from 46.5^{0}C to 48.5^{0}C leads to 16.2% reduction in the total condensation rate, i.e., 8.1% per ^{0}C. However, this ratio is higher at high temperatures. For example, as the cooling water temperature rises from 50^{0}C to 51^{0}C under identical process conditions, the total condensation rate decreases 11.7% (per ^{0}C).

NOMENCLATURE

A_{cv}	effective surface area of control volume, m^2
b	correction factor defined in Eq. (12)
BS	Baffle Spacing
c_p	specific heat, J/kg.K
F	mass transfer coefficient, kg/m^2.s
h	heat transfer coefficient, W/m^2.K
h_{ol}	heat transfer coefficient from the interface to the cooling water, W/m^2.K
$\dot{m}$	mass flow rate, kg/s
$\acute{N}_t$	condensation rate per unit area, kg/s.m^2
N_{tcc}	number of effective tube rows crossed in one cross flow section
N_{tcw}	number of tube rows crossed in the window
q	heat flux per unit area, W/m^2
R_b	bypass correction factor
R_l	leakage correction factor
R_s	end zone correction factor
Re	Reynolds number
S_m	cross flow area, m^2
S_w	window net area, m^2
T	temperature, ^{0}C
y	mole fraction

Greek Letters

ΔP_c	pressure drop in cross flow, kPa
ΔP_e	pressure drop in end zone, kPa
ΔP_i	ideal tube bank pressure drop, kPa
ΔP_w	pressure drop in baffle window, kPa
ε	Ackerman modification factor, Eq. (3)
ζ	dimensionless coordinate
λ	condensation latent heat, kJ/kg

Subscripts

c	coolant
b	gas bulk
g	steam-air mixture/non-condensable gas
i	steam condition at interface
l	condensate layer
s	steam/sensible in Eqs. (4) and (5)
v	vapor
w	window

INTRODUCTION

In the mid 1930s, Colburn and Hougen [1] and Colburn and Drew [2] were the first researchers who applied a film theory approach to condensation. As discussed by Kakaç et al. [3], Colburn and Hougen developed a solution procedure for calculating the required heat transfer area for a condenser, with one vapor stream and one non-condensable gas. The interfacial effect of the mass transfer on the heat transfer was not taken into account. This procedure was applied at many points in a condenser, and then the results were graphically integrated to determine the total area. Colburn and Drew [2] included the effects of mass transfer on the heat transfer rate and developed the transport equations for the condensation of mixed vapors.

A procedure for film theory-based condenser design was applied by Webb and Panagoulias [4] to a range of systems at atmospheric pressure. This procedure was demonstrated to work well for steam-air and mixed hydrocarbon systems. Webb and Rashtchian [5] applied this model to predict condensation of steam from air at atmospheric and reduced pressures in shell and tube condensers of standard design and industrial scale. Predictions of the effects of non-condensing gas on a condensation process were presented by the authors. Webb et al. [6] described a new approach for the design of shell-and-tube condensers, which was particularly relevant to the design of vacuum condensers. Initially an 'ideal' arrangement was calculated that could include de-superheating and gas cooling duties, in addition to the condensation itself. This 'ideal' design was used as a basis for developing a suitable arrangement of a shell and tube condenser of a standard type.

Based on the Film Theory model, Haseli and Roudaki [7] proposed a thermal rating algorithm to analyze condensation of a steam-air mixture along a baffled shell and one-path tube condenser. Very good agreement between the analytical approach and experimental data for outlet values was achieved. Haseli and Roudaki [8] extended this approach and presented a calculation method for analysis of condensation of a pure vapor in the presence of a non-condensable gas. The authors verified this method for a set of data for steam-air mixtures and water as a coolant in a counter and parallel current condenser. This method has been recently implemented by Haseli et al. [9] to study entropy production and exergy efficiency of a condenser [10].

This article aims to analyze the heat and mass transfer equations of the Film Theory to simulate condensation of steam with/without the presence of non-condensing gas, taking into account the interaction between heat and mass transfer and pressure drop in the shell-side stream.

THEORY

This section outlines the governing equations of the Film theory for describing heat and mass transfer with condensation of binary vapor mixtures, as first presented by Colburn and Drew [2]. The application of these equations is also presented for modeling thermo-hydraulic behavior of a horizontal shell and tube condenser, where condensation of steam in the presence of air takes place in the shell side. Consideration is given to the interaction between the condensation rate and pressure drop within the simulation process. In practice, failure to accurately predict the local condensation rate can lead to a significant error in estimating the pressure profile along the condensation path and vice versa.

Mass Transfer

Consider that a vapor mixture, containing a mean mole fraction y_{v1} for one of its components, flows at a temperature T_g, which is separated from the surface of a cooled solid wall by a stream of condensate. At the other side of the wall, coolant is flowing at a temperature T_c. The flux of the condensing component consists of two terms as follows:

$$\dot{N}_{t,1} = \text{(diffusive)} + \text{(convective)}$$

$$\dot{N}_{t,1} = F\frac{\partial y}{\partial \zeta} + y\dot{N}_t \qquad (1)$$

where F is the mass transfer coefficient and ζ is a dimensionless coordinate perpendicular to the surface (between 0 and 1). The total condensation rate is denoted by $\acute{N}_t$. The variable ζ represents the thickness of a thin layer near the interface between the condensate and vapor bulk, where all changes in mixture composition occur.

Solving Eq. (1) within the film layer leads to the equation of Colburn and Drew as follows:

$$\dot{N}_t = F\ln\left(\frac{z - y_i}{z - y_{v1}}\right) \qquad (2)$$

where $z = \dot{N}_{t,1} / \dot{N}_t$ and y_i is the mole fraction of vapor at the interface. If the other component of the mixture is a non-condensing gas, z is equal to unity and Eq. (2) can be written as

$$\dot{N}_t = F \ln\left(\frac{1-y_i}{1-y_{v1}}\right) \tag{3}$$

This equation was first derived by Colburn and Hougen [1].

Heat Transfer

The local heat flux absorbed by the coolant consists of two quantities: sensible heat and latent heat. The first term is the sum of two terms itself: sensible heat due to cooling the bulk and sensible heat of cooling the condensed vapor, separated from the bulk transferred to the interface. In terms of symbols, this may be expressed as follows:

$$q_s = h_g \frac{dT_g}{d\zeta} + \dot{N}_t c_{pv}\left(T_g - T_i\right) \tag{4}$$

where h_g is the heat transfer coefficient of the gas, c_{pv} is the specific heat of the vapor and T_i is the interface temperature. The solution for Eq. (4) with boundary conditions $\zeta=0$, $T_g=T_i$ and $\zeta=1$, $T_g=T_g$ becomes

$$q_s = h_g \varepsilon\left(T_g - T_i\right) \tag{5}$$

where ε denotes the Ackermann modification factor, which accounts for the flow of heat associated with the mass transfer across the film [3], as defined by

$$\varepsilon = \frac{\left(\dot{N}_t c_{pv}/h_g\right)}{1-\exp\left(-\dot{N}_t c_{pv}/h_g\right)} \tag{6}$$

In addition, latent heat due to condensation can be written as follows:

$$q_\lambda = \dot{N}_t \lambda \tag{7}$$

where λ is the condensation latent heat. One may now write the heat balance of the system as

$$h_{ol}\left(T_i - T_w\right) = h_g \varepsilon\left(T_g - T_i\right) + \dot{N}_t \lambda \tag{8}$$

where h_{ol} is the heat transfer coefficient from the interface to the coolant.

MODELING

This section will show how to apply the *Film Theory* equations to simulate heat and mass transfer in a shell-and-tube exchanger. Condensation of a pure vapor takes place with/without the presence of a non-condensing gas in the shell side, with coolant flowing through the tubes. Figure 1 depicts schematically the configuration of a condenser to be modeled, which is a TEMA 'E' shell with one-path tube. Vapor mixed with some percentage of non-condensable gas enters the condenser at one end and flows across tubes in each baffle space. As it flows through the baffle spaces, condensation takes place due to contact with the cooling wall of the tubes along the heat exchanger, until the last baffle space where uncondensed vapor and non-condensable gas are extracted. Figure 1 shows a counter-current configuration. Flow of coolant inside the tubes occurs in the opposite direction of the main flow of the mixture. Select an arbitrary control volume such as that shown in Fig. 1, to derive the related conservation laws of energy and mass balances for the shell and tube sides. The condensation temperature is postulated to be unique within the control volume, and represented by T_i.

Shell Side Conservation Laws

It is assumed that all changes in temperature, composition and pressure occur in the direction of the flowing mixture, normal to the tubes. Assuming that the mixture bulk cools down from T_{g1} to T_{g2} due to only convective heat transfer, the following differential equation may be derived for the energy conservation in the bulk side of the mixture,

$$\dot{m}_b c_{pb} dT_b = -h_g b\left(T_b - T_i\right) dA \tag{9}$$

where the subscript b represents the bulk and

$$\dot{m}_b = \overline{\dot{m}}_v + \dot{m}_g \tag{10}$$

where $\overline{\dot{m}}_v$ is the mean mass flow rate of vapor in the control volume. It is worth noting that the heat transfer coefficient h_g is modified by a correction factor *b* instead of the Ackermann modification factor, ε, introduced in Eq. (5) and defined by Eq. (6). The sensible heat due to cooling of condensed vapor (second term on the right hand side of Eq. (4)) should be subtracted from the total sensible heat. Hence, it may be shown that

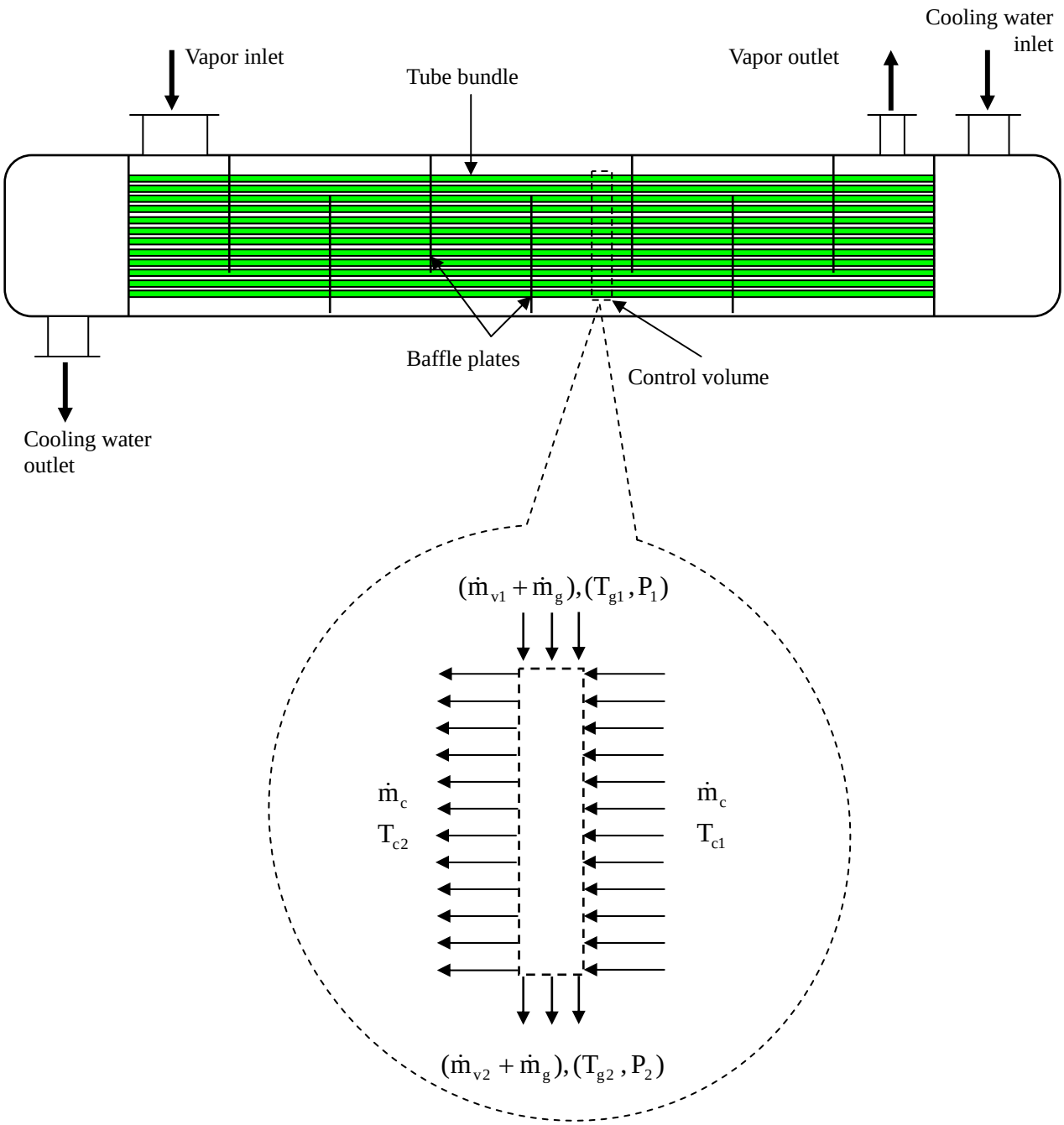

FIG. 1: SCHEMATIC OF THE CONDENSER AND AN ARBITRARY CONTROL VOLUME

$$b = \frac{\left(\dot{N}_t c_{pv} / h_g\right)}{\exp\left(\dot{N}_t c_{pv} / h_g\right) - 1} \tag{11}$$

Integrating Eq. (9) with (A=0, $T_b=T_{g1}$) and ($A=A_{cv}$, $T_b=T_{g2}$) as boundary conditions leads to the following temperature drop of the mixture bulk:

$$\Delta T_b = \left(T_{g1} - T_i\right)\left[1 - \exp\left(\frac{h_g b}{\dot{m}_b c_{pb}} A_{cv}\right)\right] \tag{12}$$

Furthermore, the flow rate of vapor reduces from $\dot{m}_{v1}$ to $\dot{m}_{v2}$ due to condensation.

The following differential equation represents the conservation of mass of the shell side.

$$\frac{d\dot{m}_v}{dA} = -\dot{N}_t \tag{13}$$

Integrating Eq. (13) over an effective heat and mass transfer area, A_{cv}, yields

$$\Delta\dot{m}_v = -\overline{\dot{N}}_t A_{cv} \tag{14}$$

This expresses the net change in vapor mass flow rate, i.e., the condensation rate. In Eq. (14), the mean mass transfer due to condensation within a control volume is represented by $\overline{\dot{N}}_t$.

Shell Side Pressure Drop

Note that the shell side pressure strongly affects the condensation (saturation) temperature of the vapor, so that it influences the driving temperature force and rate of heat transfer over the interface. Three distinct sources of pressure drop have been taken into consideration, as documented by Taborek [11] in the Heat Exchanger Design Handbook: (1) pressure drop in cross-flow between the baffle tips, ΔP_c, (2) pressure drop in the baffle window, ΔP_w, and (3) cross-flow pressure drop in the end zones (first and last BS), ΔP_e:

$$\Delta P_c = \Delta P_i . R_b R_l \tag{15}$$

$$\Delta P_w = \left[\left(2 + 0.6 N_{tcw}\right)\frac{\left(\dot{m}_w\right)^2}{2\rho_g}\right].R_l \qquad Re_g \geq 100 \tag{16}$$

$$\Delta P_e = \Delta P_i\left(1 + \frac{N_{tcw}}{N_{tcc}}\right).R_b.R_s \tag{17}$$

where ΔP_i is the ideal tube bank pressure drop, and R_b, R_l and R_s denote, respectively, bypass, leakage and end zone correction factors. Also, N_{tcw} refers to the number of tube rows crossed in the window, whereas N_{tcc} represents the number of effective tube rows crossed in one cross flow section, i.e., between the baffle tips. Also,

$$\dot{m}_w = \frac{\dot{m}_g}{\sqrt{S_m S_w}} \tag{18}$$

where S_m and S_w account for the cross-flow area and the window net area, respectively.

Tube Side Energy Conservation

It is postulated that the temperature gradient in the direction of the coolant flow is more significant than its change in the mixture direction. Neglecting the latter change in coolant temperature, the increase in coolant temperature occurs due to the convective heat transfer because of the temperature difference between the interface and coolant bulk. Hence,

$$\dot{m}_c c_{pc} dT_c = h_{ol}\left(T_i - T_c\right)dA \tag{19}$$

Integration of Eq. (19) within a control volume shown in Fig. 1 results in the following expression for augmentation of the coolant temperature across the control volume

$$\Delta T_c = \left(T_i - T_{c2}\right)\left[1 - \exp\left(\frac{h_{ol}}{\dot{m}_c c_{pc}} A_{cv}\right)\right] \tag{20}$$

MODEL VALIDATION

In this section, the numerical solution will be determined from the modeling methodology described in the previous section, based on heat and mass transfer

equations of Film Theory. For validation purposes, past experimental data of Webb et al. [12], taken from an industrial scale heat exchanger, are employed. Webb and co-workers [12] measured an extensive set of experimental data involving condensation of steam and steam-air mixtures at atmospheric and reduced pressures, in TEMA 'E' shell and 'J' shell condensers. A typical reported set of measured performance parameters of a TEMA 'E' shell condenser, for the case of pure steam, is given in Table 1. Geometrical specifications of the condenser are tabulated in Table 2.

TABLE 1: INLET VALUES OF PROCESS PARAMETERS

Pressure (kPa)	22.9
Steam Temperature (^{0}C)	62.94
Steam Mass Flow Rate (kg/min)	20.7
Cooling Water Temperature (^{0}C)	47.63
Cooling Water Mass Flow Rate (kg/s)	43.45

TABLE 2: GEOMETRICAL SPECIFICATION OF THE CONDENSER IN REF. [12]

Shell Inside Diameter (mm)	356
Tube Outside Diameter (mm)	19.08
Tube Pitch (mm)	25.4
Tube Length (m)	2.46
Layout Angle (deg)	30
Baffle Cut (% of Shell Diameter)	37
Inlet Baffle Spacing Length (mm)	426
Outlet Baffle Spacing Length (mm)	426
Central Baffle Spacing Length (mm)	268
Total Tube Number	106

The current formulation is applied to each baffle space (BS). Thus, the calculation is started from the first BS where steam enters the exchanger, and carried out towards the last one. It is assumed that for any BS like BS_k, inlet values of the shell fluid temperature $T_{g,k}$, steam mass rate $\dot{m}_{s,k}$ and cooling water temperature $T_{c,k}$ are known. Using Eqs. (12), (14) and (20), the calculation proceeds to determine the values of these terms at the outlet of the BS_k, i.e. $T_{g,k+1}$, $\dot{m}_{s,k+1}$ and $T_{c,k+1}$ respectively, which will be the inlet values for the next BS. A solution of Eqs. (12), (14) and (20) depends upon knowing the local values of the condensation temperature, T_i, and condensation rate, $\acute{N}_t$. Therefore, one must first solve simultaneously Eqs. (3) and (8) by trial-and-error to determine their values. A past study of Haseli and Roudaki [8] includes two methods of solutions which quickly converge with respect to the values of T_i and $\acute{N}_t$. After temperature gradients of both the shell side and tube side, as well as the condensation rate within a given BS, have been found, the pressure drop of the shell side is calculated, as described previously.

The overall predicted condenser performance for the data given in Tables 1 and 2 is compared with experimental values in Table 3. Excellent agreement between the results of simulations and measured values is seen from Table 3 for the outlet temperatures, condensation rate and total pressure drop. The resulting temperature and pressure profiles along the condenser are depicted in Fig. 2. The temperature drop of vapor occurs due to the pressure drop, which directly influences the condensation temperature. A similar observation was also reported by Webb et al. [12]. When steam condenses along the heat exchanger, its mass flow rate reduces. Hence, the heat transfer coefficient and pressure drop decrease as condensation proceeds, as both are functions of the vapor velocity. The rate of condensation and pressure drop are high in the first few BSs, since the vapor velocity is high at the entrance BSs. Figure 2 illustrates the predicted pressure drop.

TABLE 3: COMPARISON BETWEEN PREDICTED AND EXPERIMENTAL VALUES (PURE STEAM)

	Predicted	Experiment	Difference (%)
Total Pressure Drop (kPa)	4.41	4.68	5.8
Outlet Steam Temperature (^{0}C)	59.79	58.48	2.2
Outlet Steam Mass Flow Rate (kg/min)	2.45	2.35	4.3
Total Condensation Rate (kg/min)	18.25	18.35	0.5
Outlet Cooling Water Temperature (^{0}C)	51.59	51.57	-

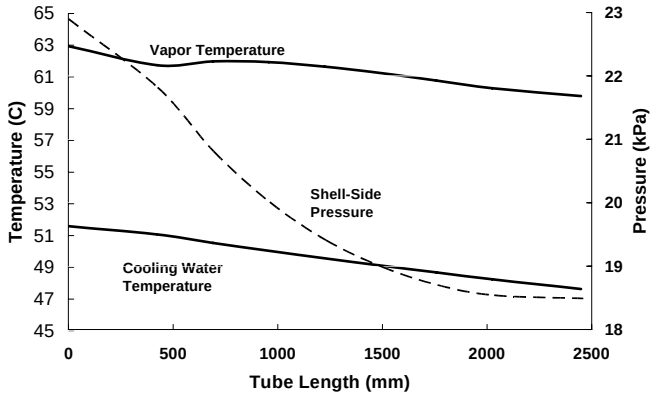

FIG. 2: PREDICTED PROFILES OF TEMPERATURE AND PRESSURE ALONG THE CONDENSER (PURE VAPOR)

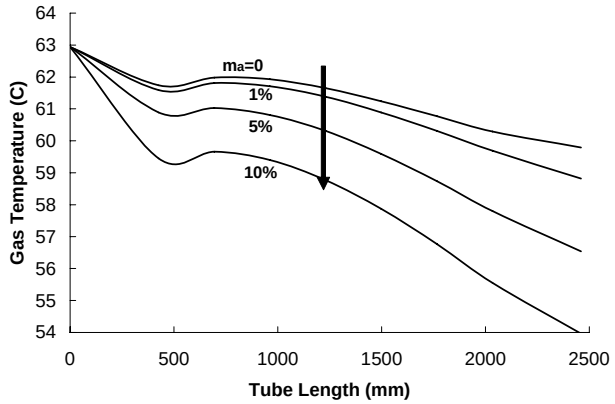

(a)

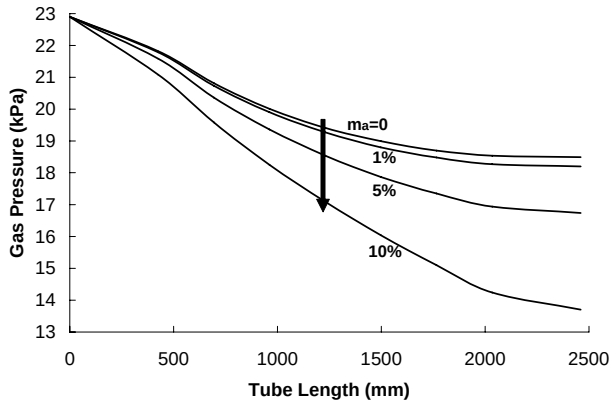

(b)

FIG. 3: EFFECTS OF AIR LEAKAGE ON SHELL-SIDE GAS (a) TEMPERATURE AND (b) PRESSURE

RESULTS AND DISCUSSION

An important aspect of the condensation process is the influence of non-condensing gas on the heat and mass transfer rates. An advantage of the current model is that in addition to the case of pure vapor, the effects of the presence of non-condensing gas on the condensation process can be taken into consideration. The accuracy of the current formulation is further validated by generating temperature and pressure profiles at various air leakages, as a percentage of the upstream steam mass flow rate. Figure 3 illustrates the resulting graphs. Air adds a heat and mass transfer resistance and therefore reduces the rate of condensation of the vapor. The existence of air significantly influences the condensation temperature, since the partial pressure of vapor is affected. Thus, as condensation takes place within the BSs, the vapor bulk and condensation temperatures decrease as air accumulates along the condenser (Fig. 3a). On the other hand, from Fig. 3b, the presence of air results in a higher pressure drop on the gas side. As noted previously, this is due to less condensation at a higher air leakage percentage, so that a higher pressure drop takes place, since the pressure is proportional to the square of the gas flow rate. Figure 4 illustrates the effect of the presence of air on the gas side temperature and pressure drops, as well as the total condensation rate. From this figure, the total condensation rate decreases 5% and 20.5%, at an air leakage of 1% and 5%, respectively, compared to the situation of pure vapor.

Furthermore, the inlet cooling water temperature is an important process parameter that influences the condensation process. Similarly, the total amounts of process parameters such as those shown in Fig. 4 are evaluated at different inlet cooling water temperatures. The results are shown in Fig. 5. The resultant profiles at different inlet cooling water temperatures are similar to those shown in Fig. 4 for various air leakages. A higher drop in gas side temperature and pressure, and lower condensation rate, may also result from increasing the inlet cooling water temperature. As the cooling water temperature rises, the effective driving temperature force decreases. Thus, the rates of heat and mass transfer decrease. Since condensation takes place slowly, the vapor flow rate is higher at warmer cooling water conditions. It results in a higher pressure drop due to both major sources of pressure drop, which occur in cross-flow and the baffle window. It can be observed from Fig. 5 that increasing the inlet cooling water temperature from 46.5^0C to 48.5^0C leads to a 16.2% reduction in the total condensation rate, i.e. 8.1% per ^{0}C. However, this ratio is higher at high temperatures. For instance, as the cooling water temperature rises from 50^0C to 51^0C (under identical process conditions), the total condensation rate decreases by 11.7% (per ^{0}C).

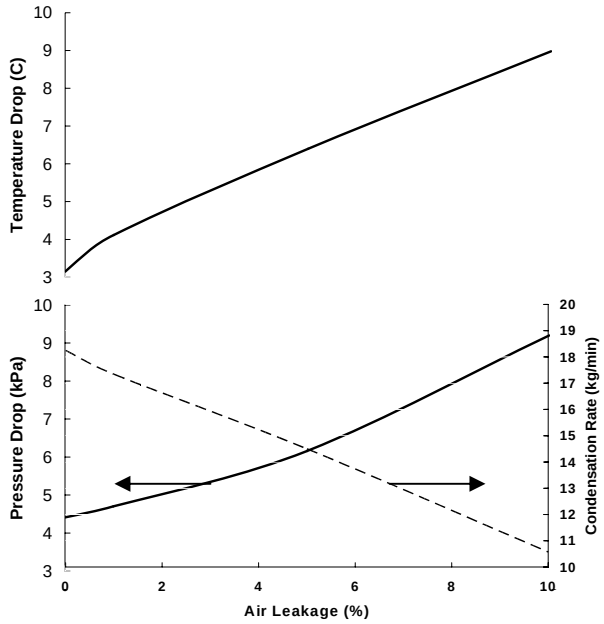

FIG. 4: EFFECTS OF AIR LEAKAGE ON TOTAL TEMPERATURE DROP, PRESSURE DROP AND CONDENSATION RATE

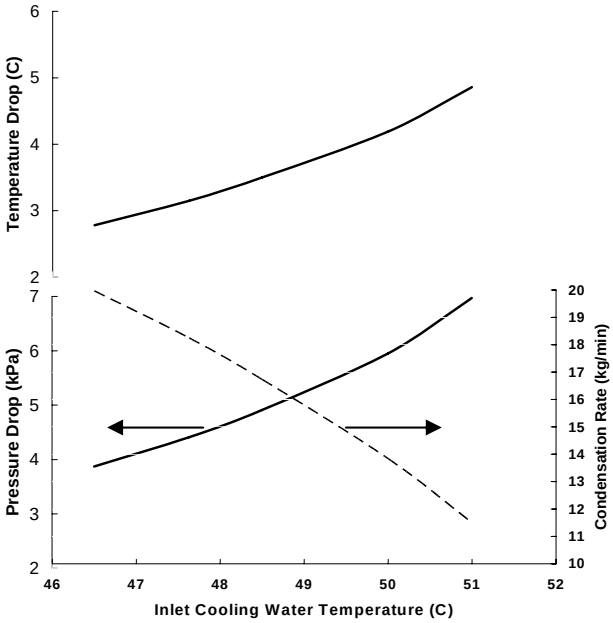

FIG. 5: EFFECTS OF INLET COOLING WATER TEMPERATURE ON TOTAL TEMPERATURE DROP, PRESSURE DROP AND CONDENSATION RATE

CONCLUSIONS

A mathematical model has been developed based on Film Theory heat and mass transfer equations, to predict condensation of steam. It takes into account the effects of a non-condensing gas, i.e. air, within a shell-and-tube condenser. The interaction of heat and mass transfer with shell-side hydrodynamics is also taken into consideration. The advantage of this new formulation is its capability to accurately predict the condensation process, with or without the presence of air. The performance predictions for a typical condenser agree very well with experimental measurements. Moreover, by investigating the effects of air leakage and cooling water temperature on various process parameters, i.e., changes of gas temperature, pressure and total condensation rate, the accuracy of the present model is further validated.

ACKNOWLEDGMENTS

The authors acknowledge the financial support provided by the Ontario Research Excellence Fund.

REFERENCES

1. A. P. Colburn, O. A. Hougen, Design of cooler condensers for mixtures of vapours with non-condensing gases, Ind. Eng. Chem. 26 (1934) 1178-1182.
2. A. P. Colburn, T. B. Drew, The condensation of the mixed vapours, Transaction of American Institute of Chemical Engineers 33 (1937) 197-215.
3. S. Kakaç, A. E. Bergles, E. O. Fernandes, Two-Phase Flow Heat Exchanger, NATO ASI Series, 1987, Kulwer Academic Publishers.
4. D. R. Webb, D. Panagoulias, An improved approach to condenser design using film method, International Journal of Heat and Mass Transfer 30 (2) (1987) 373-378.
5. D. Rashtchian, D. R. Webb, Condensation of steam from mixtures with air in a shell and tube exchanger at atmospheric and reduced pressures, Chemical Engineering Research and Design 65 (2) (1987) 157-164.
6. D. R. Webb, R. Bird; K. Mangnall, New approach to design of vacuum condensers, Chemical Engineering Research and Design 67 (6) (1989) 639-649.
7. Y. Haseli, S. J. M. Roudaki, Simultaneous modeling of heat and mass transfer of steam-air mixture on a shell and tube condenser based on film theory, Proceedings of the ASME Summer Heat Transfer Conf., 2003, Las Vegas, NV, Vol. 2, pp 251-259.
8. Y. Haseli, S. J. M. Roudaki, A calculation method for analysis condensation of a pure vapor in the presence of a non-condensable gas on a shell and tube condenser, Proceedings of the ASME Heat Transfer/Fluids Engineering Summer Conf., 2004, Charlotte, NC, Vol. 3, pp 155-163.

9. Y. Haseli, I. Dincer, G. F. Naterer, Entropy generation number for condensation of a vapor in the presence of a non-condensable gas in a shell and tube condenser, International Journal of Heat and Mass Transfer (2007) (In press).
10. Y. Haseli, I. Dincer, F. G. Naterer, Exergy analysis of condensation of a binary mixture with one non-condensable component in a shell and tube condenser, ASME Journal of Heat Transfer (2008) (in press).
11. J. Taborek, Shell and tube heat exchangers, Heat Exchanger Design Handbook, Vol. 3, Chap. 3, Hemisphere, Washington DC, 1983.
12. D. R. Webb, A. J. Dell, J. Williams, R. W. Stevenson, An experimental comparison of the performance of TEMA 'E' and 'J' shell condensers, Chemical Engineering Research and Design 75 (1997) 646-651.